

# A RATIONAL APPROXIMATION METHOD FOR THE NONLINEAR EIGENVALUE PROBLEM

YOUSSEF SAAD <sup>\*</sup>, MOHAMED EL-GUIDE <sup>†</sup>, AND AGNIESZKA MIEDLAR <sup>†</sup>

**Abstract.** This paper presents a method for computing eigenvalues and eigenvectors for some types of nonlinear eigenvalue problems. The main idea is to approximate the functions involved in the eigenvalue problem by rational functions and then to linearize the resulting problem. A few different schemes are proposed to solve this linear eigenvalue problem. The expanded form of the linear problem is not solved directly but it is exploited instead to extract all eigenvalues in a certain region of the complex plane. A few theoretical results are established to explain why the approach works and a few numerical experiments are described to validate it.

**Key words.** Nonlinear eigenvalue problem, Rational approximation, Cauchy integral formula, FEAST eigensolver.

**1. Background and introduction.** We consider the nonlinear eigenvalue problem (NLEVP)

$$T(\lambda)u = 0, \quad (1.1)$$

where  $T(z) \in \mathbb{C}^{n \times n}$  is a holomorphic matrix-valued function on an open set  $\Omega \subseteq \mathbb{C}$  that is nonlinear in the parameter  $z$ . There are many differences between the linear case where  $T(z) = A - zB$  and the general nonlinear case. For example, the number of eigenvalues of  $T$  is no longer equal to  $n$  but can be arbitrary and eigenvectors associated with distinct eigenvalues are not necessarily linearly independent.

Problems of this type arise in many applications, e.g., in fluid-structure interaction problems [51], acoustic problems with absorbing boundary conditions [9] or in electronic structure calculation for quantum dots [5]. Sometimes the underlying nonlinear eigenvalue problems may be dependent not only on the spectral parameter but also on some additional physical parameters and need to be solved for a large parameter range, e.g., describing vibration behavior of viscoelastic materials leads to NLEVPs with stiffness properties which are frequency-dependent [9], whereas band structure calculations for photonic crystals result in problems that depend on the wave vector [20]. The following provides a brief introduction to the numerical treatment of NLEVPs. More comprehensive surveys on the state of the art in NLEVPs can be found in [48, 27, 54, 26, 16].

*Newton-type methods.* A classical algorithm for solving general nonlinear eigenvalue problems is to exploit a Newton method to find the zeros of the characteristic equation  $\det(T(\lambda)) = 0$ , see e.g., the Newton-trace iteration [23, 24], Newton-QR method [22] or implicit determinant method [44]. Alternatively, the Newton method can be applied to the vector equation

$$F(x, \lambda) = \begin{bmatrix} T(\lambda)x \\ c^H x - 1 \end{bmatrix} = 0, \quad (1.2)$$

where  $c \in \mathbb{C}^n$  is a suitably chosen normalization vector. The Newton iteration step for (1.2) results in the *nonlinear inverse iteration* method [49, 34]. The inverse iteration

---

<sup>\*</sup>Address: Computer Science & Engineering, University of Minnesota, Twin Cities. Work supported by NSF grant 1812695. e-mail: [{saad, melguide}@umn.edu](mailto:{saad, melguide}@umn.edu)

<sup>†</sup>University of Kansas, Dept. of Mathematics. Work supported by NSF grant 1812927. e-mail: [amiedlar@ku.edu](mailto:amiedlar@ku.edu)

method can be extended using (generalized) Rayleigh functional to the *Rayleigh functional iteration* method [33] in the case of Hermitian  $T(\cdot)$ , or the *two-sided Rayleigh functional iteration* [40] for the general  $T(\cdot)$ . All the above mentioned variants of inverse iteration require factoring the matrix  $T(\lambda_k)$  at each step step  $k$ . To overcome this difficulty, Neumaier [31] proposed the *residual inverse iteration*.

For simple eigenpairs, single vector Newton-like methods, i.e., inverse iteration, Rayleigh functional iteration, residual inverse iteration or single-vector Jacobi-Davidson [31, 18, 12] as well as their inexact counterparts [45, 46] exhibit local quadratic or cubic (in the presence of symmetry of  $T(\cdot)$ ) convergence. Another Newton-type method based on the first order approximation of problem (1.1) is the method of *successive linear problems (linear approximations)* [34]. If one can provide a variational characterization of eigenvalues, the nonlinear eigenvalue problem can also be solved by the so-called *safe-guarded iteration method* [55, 53]. In principle, all presented methods can be used to compute several eigenpairs if combined with deflation techniques, e.g., using nonequivalence transformation to map the already computed eigenvalues to infinity [16] or invariant pairs [10]. The block analog of Newton method for computing an invariant pair of  $T(\cdot)$  is presented in [21]. The complementary sensitivity of invariant pairs is discussed in [47].

*Methods based on contour integration.* In a series of papers Asakura et al. introduced nonlinear variants of the Sakurai-Sugiura (SS) method [39] with block Hankel matrices (SS-H method) for the polynomial eigenvalue problems [1] and for eigenvalue problems with analytic matrix-valued functions  $T(\lambda)$  [2]. Although cost- efficient and scalable, the method yields solutions with relatively low accuracy. Almost at the same time, Beyn [8] introduced a contour integration technique that allows to reduce a NLEVP with  $m \ll n$  eigenvalues inside contour  $\Gamma$  to solving a linear eigenvalue problem of dimension  $m$ . The main idea of Beyn's integral method is to probe a Jordan decomposition of the  $m \times m$  matrix following the Keldysh's theorem [29, Theorem 1.6.5]. The method is conceptually simple but probing a Jordan decomposition is known to be extremely sensitive to perturbations. Moreover, since the value of the parameter  $m$  (the number of linearly independent eigenvectors) is not known in advance, the practical realization of Beyn's algorithm requires various adaptations. For example, refining the accuracy of the contour integration for a single multiplication involves performing a new matrix factorization for each newly added quadrature point, making its overall computational cost relatively high. Also the numerical quadrature errors in the contour integral can significantly impact the accuracy of the results.

Recently, Yokota and Sakurai [56] addressed the problem of low accuracy in the nonlinear SS-H method by using the Rayleigh-Ritz procedure to extract the approximate eigenpairs from the underlying subspaces. The resulting projection-type method does not require any fixed point iterations and gives better accuracy than the methods of Asakura et al. [1] and Beyn [8]. In comparison to Beyn's integral approach, the SS-type methods refine their solutions by increasing the dimension of their search subspaces by calculating additional moments of (1.3) using the same quadrature rule each time; the dimension of the search subspace is increased iteratively until the desired solution is sufficiently accurate. All contour integral methods mentioned above exploit the moments of the Cauchy integral of the residual function  $T(\lambda)$ , i.e.,

$$\frac{1}{2\pi i} \oint_{\Gamma} z^k T^{-1}(z) dz, \quad k \geq 0, \quad (1.3)$$

and can be easily obtained as an algorithmic realization of the general framework presented in [16, Theorem 5.2]. Beyn's method uses the zeroth ( $k = 0$ ) and first ( $k =$

1) moments, whereas the SS-type methods use a number of moments  $k$  as large as is necessary to reach convergence. Eigenvalue techniques based on higher-order moments are necessary when  $m > n$  and the generalized eigenvectors are not necessarily linearly independent. A new efficient and highly-parallelizable contour integral method based on an alternate integrand function has been recently introduced in [14]. The nonlinear FEAST algorithm is a generalization of Neumaier's [31] residual inverse iteration using multiple shifts and it allows to compute eigenpairs corresponding to the eigenvalues that lie in an arbitrary user-specified region in the complex plane.

*Other methods.* As for the linear eigenvalue problems involving large and sparse matrices, iterative projection methods have been found useful for solving their nonlinear counterparts. The nonlinear Arnoldi method [52] does not generate a Krylov subspace as does its linear predecessor, but it still allows to transform the large-scale problem to the one of much smaller dimension. Other Arnoldi-type methods have been proposed, e.g., a second-order Arnoldi method [3] or two-level orthogonal Arnoldi method [25]. Jacobi-Davidson methods provide an alternative to Arnoldi-type methods and have been extensively studied in various contexts [42, 7, 41]. Another class of linearization-based approaches consists of methods like Chebyshev interpolation method [11], infinite Arnoldi and bi-Lanczos methods [19, 13] and rational Krylov methods [36, 37, 32, 15, 4, 50].

When dealing with large-scale nonlinear eigenvalue problems many of the approaches just mentioned involve two main steps: (1) projecting the large-scale nonlinear eigenvalue problem onto a subspace of small dimension, (2) solving the resulting small, still nonlinear, eigenvalue problem. We will refer to a technique of this type as a *nonlinear projection method*.

The goal of this paper is to introduce a new class of methods for solving nonlinear eigenvalue problems. We begin by restricting slightly the class of problems we consider. Specifically, we follow Kressner [21] and limit ourselves to problems in which:

$$T(z) = f_0(z)A_0 + f_1(z)A_1 + f_2(z)A_2 + \dots + f_p(z)A_p, \quad (1.4)$$

with holomorphic functions  $f_0, \dots, f_p : \Omega \rightarrow \mathbb{C}$  and constant coefficient matrices  $A_0, \dots, A_p$ . In what follows we will call  $\Gamma$  the boundary of  $\Omega$ . Since  $T \in H(\Omega, \mathbb{C})$ , it can always be written in the form (1.4) with at most  $p = n^2$  terms. Note also that this representation is not unique. Furthermore, it is very common in practice to have  $f_0(z) = 1$  and  $f_1(z) = z$ , so instead of the above we will assume the form:

$$T(z) = -B_0 + zA_0 + f_1(z)A_1 + \dots + f_p(z)A_p. \quad (1.5)$$

As it turns out many of the nonlinear eigenvalue problems encountered in applications are set in this form. We are interested in all eigenvalues that are located in a region of the complex plane enclosed by curve  $\Gamma$ .

The techniques introduced in this paper are all based on first replacing the original problem by one in which the nonlinear functions  $f_j(z)$  are approximated by rational functions. Once this transformation is performed, it is possible to solve the resulting problem directly by linearization and this can be adequate for small problems. For larger problems, we also propose a *nonlinear* projection-type method of the type discussed above.

The next section will introduce the idea of rational approximation for solving problems of type (1.5) along with several algorithms. Section 3 presents some theoretical results. Numerical experiments are discussed in Section 4 and a few concluding remarks are stated in Section 5.

**2. Rational approximation methods for NLEVPs.** The main assumption we make is that each of the holomorphic functions  $f_j : \Omega \rightarrow \mathbb{C}$  in representation (1.5) is well approximated by a rational function of the form:

$$f_j(z) = \sum_{i=1}^m \frac{\alpha_{ij}}{z - \sigma_i}. \quad (2.1)$$

Note that the set of poles  $\sigma_i$ 's is the same for all of the functions. This setting comes from a Cauchy integral representation of each function inside a region limited by a contour  $\Gamma$ :

$$f_j(z) = -\frac{1}{2i\pi} \int_{\Gamma} \frac{f_j(t)}{z - t} dt, \quad z \in \Omega. \quad (2.2)$$

Using numerical quadrature (2.2) is then approximated into (2.1), where the  $\sigma_i$ 's are quadrature points located on the contour  $\Gamma$ . Substituting (2.1) into (1.5) yields the following approximation  $\tilde{T}$  of  $T$ :

$$\begin{aligned} \tilde{T}(z) &= -B_0 + zA_0 + \sum_{j=1}^p \sum_{i=1}^m \frac{\alpha_{ij}}{z - \sigma_i} A_j = -B_0 + zA_0 + \sum_{i=1}^m \frac{\sum_{j=0}^p \alpha_{ij} A_j}{z - \sigma_i} \\ &\equiv -B_0 + zA_0 + \sum_{i=1}^m \frac{B_i}{z - \sigma_i}, \end{aligned} \quad (2.3)$$

where we have set

$$B_i = \sum_{j=0}^p \alpha_{ij} A_j, \quad i = 1, \dots, m. \quad (2.4)$$

Given the approximation  $\tilde{T}(z)$  of  $T(z)$  shown in (2.3), the problem we need to solve can be written as follows:

$$\left( -B_0 + zA_0 + \sum_{i=1}^m \frac{B_i}{z - \sigma_i} \right) u = 0. \quad (2.5)$$

We will often refer to this problem as a *surrogate* for problem (1.5). It will be seen that if each of the functions  $f_j$  is well approximated then this surrogate problem will provide good approximations to eigenvalues of (1.5) located inside the contour but that are not close to the poles.

For a given vector  $u$ , let us define

$$v_i = \frac{u}{\sigma_i - z}, \quad i = 1, \dots, m. \quad (2.6)$$

Then we can write

$$\tilde{T}(z)u = \left( -B_0 + zA_0 + \sum_{i=1}^m \frac{B_i}{z - \sigma_i} \right) u \quad (2.7)$$

$$= (-B_0 + zA_0)u - \sum_{i=1}^m B_i v_i, \quad (2.8)$$

which can be expressed in block form as follows:

$$\begin{bmatrix} (z - \sigma_1)I & & & I \\ & (z - \sigma_2)I & & I \\ & & \ddots & \vdots \\ & & & (z - \sigma_m)I & I \\ -B_1 & -B_2 & \dots & -B_m & zA_0 - B_0 \end{bmatrix} w = 0, \quad w = \begin{bmatrix} v_1 \\ v_2 \\ \vdots \\ v_m \\ u \end{bmatrix}. \quad (2.9)$$

Since (2.9) is of the form  $(z\mathcal{M} - \mathcal{A})w = 0$ , solutions of the surrogate eigenvalue problem  $\tilde{T}(\lambda)u = 0$  can be obtained by solving the linear eigenvalue problem

$$\mathcal{A}w = \lambda\mathcal{M}w, \quad (2.10)$$

with

$$\mathcal{M} = \begin{bmatrix} I & & & \\ & I & & \\ & & \ddots & \\ & & & \ddots \\ & & & & A_0 \end{bmatrix}, \quad \mathcal{A} = \begin{bmatrix} \sigma_1 I & & & -I \\ & \sigma_2 I & & -I \\ & & \ddots & \vdots \\ & & & \sigma_m I & -I \\ B_1 & B_2 & \dots & B_m & B_0 \end{bmatrix}. \quad (2.11)$$

Note that the diagonal block with the  $\sigma_i$ 's is of dimension  $(mn) \times (mn)$  and the matrices  $\mathcal{M}$ , and  $\mathcal{A}$  are each of dimension  $(mn+n) \times (mn+n)$ . The above formalism provides a basis for developing algorithms to extract approximate eigenvalues of the original problem (1.5) but note that we will not store the matrices  $\mathcal{A}$  and  $\mathcal{M}$  explicitly.

**2.1. Shift-and-invert on full system.** We will now consider a subspace iteration or an Arnoldi-type procedure for solving problem (2.10 – 2.11). Partial solutions of the problem can be extracted by several available algorithms. Since we are interested in interior eigenvalues, it is imperative to exploit a shift-and-invert strategy, which consists of replacing the solution of problem (2.10) by

$$\mathcal{H}w = \frac{1}{\lambda - \sigma}w, \quad \mathcal{H} := (\mathcal{A} - \sigma\mathcal{M})^{-1}\mathcal{M}, \quad (2.12)$$

where  $\sigma$  is a certain shift.

In order to extract the eigenvalues closest to the specified shift  $\sigma$ , we will use the Arnoldi or subspace iteration method to compute the *dominant* eigenvalues of (2.12). These two projection procedures will require solving linear systems with a shifted matrix  $(\mathcal{A} - \sigma\mathcal{M})$  at each step. To solve such systems, we can exploit a standard block LU factorization that takes advantage of the specific patterns of  $\mathcal{A}$  and  $\mathcal{M}$ . As a consequence of (2.11), all these systems are of the form

$$\begin{bmatrix} D & F \\ B^T & B_0 \end{bmatrix} \begin{bmatrix} x \\ y \end{bmatrix} = \begin{bmatrix} a \\ b \end{bmatrix}, \quad (2.13)$$

where  $D$  is diagonal. Consider the block LU factorization of matrix  $\mathcal{A}$ :

$$L = \begin{bmatrix} I & 0 \\ B^T D^{-1} & I \end{bmatrix}, \quad U = \begin{bmatrix} D & F \\ 0 & S \end{bmatrix}, \quad (2.14)$$

where  $S = B_0 - B^T D^{-1}F$  is the Schur complement of the block  $B_0$ . Solving (2.13) requires first solving the system  $Sy = b - B^T D^{-1}a$  and then substituting  $y$  in the first part of (2.13) to obtain  $x = D^{-1}(a - Fy)$ . This results in a practical algorithm sketched as Algorithm 1 below. As explained earlier, the linear system solves involved in line 2 of Algorithm 1 are processed without forming the matrices  $\mathcal{A}, \mathcal{M}$  explicitly.

---

**Algorithm 1:** Shift-and-Invert Arnoldi on full system (2.10)

---

**Input :** A matrix-valued function  $T(\lambda) \in \mathbb{C}^{n \times n}$ , shift  $\sigma$ , number of eigenvalues  $k$ , number of quadrature nodes  $m$  for the rational approximations (2.1)

**Output:**  $\lambda_1, \dots, \lambda_k, U_k$

- 1 Compute  $B_i, i = 1, \dots, m$  from (2.4);
- 2 Compute the  $k$  largest eigenvalues closest to  $\sigma$  using Implicitly Restarted Arnoldi method applied to matrix  $\mathcal{H}$  in (2.12);
- 3 **return**  $\lambda_1, \dots, \lambda_k$  and eigenvector matrix  $U_k$

---

**2.2. Power iteration and full Subspace Iteration.** We now examine carefully the iterates of the inverse power method (inverse iteration) or shift-and-invert method to see how they can be integrated into a subspace iteration approach. For simplicity, we will assume for now that  $A_0 = I$ . We write the iterates obtained from an inverse iteration procedure as  $w^{(j)} = [v^{(j)} ; u^{(j)}]$  where we used MATLAB notation  $[x ; y]$  to denote a vector that consists of  $x$  stacked above  $y$ . We begin by discussing the inverse power method (inverse iteration).

*Inverse power method.* Each step of the inverse power method (inverse iteration) requires solving the linear system

$$\mathcal{A}w^{(j+1)} = w^{(j)} \quad \text{or} \quad \mathcal{A} \begin{bmatrix} v^{(j+1)} \\ u^{(j+1)} \end{bmatrix} = \begin{bmatrix} v^{(j)} \\ u^{(j)} \end{bmatrix}, \quad (2.15)$$

and scaling the new vector in a certain way, see e.g., [38, Sec. 4.1]. In the case of shift-and-invert method the matrix  $\mathcal{A}$  is replaced by  $\mathcal{A} - \sigma I$  where  $\sigma$  is the shift, but the rest of the approach stays identical - so we assume that  $\sigma = 0$ . The system (2.15) is of the same form as that in (2.13) and it can be solved the same way, resulting in the following steps (assuming  $\sigma = 0$ ):

$$u^{(j+1)} = S^{-1}(u^{(j)} - B^T D^{-1} v^{(j)}), \quad (2.16)$$

$$v^{(j+1)} = D^{-1}(v^{(j)} - F u^{(j+1)}). \quad (2.17)$$

Algorithm 2 shows an implementation of a single step of this scheme for a general  $\sigma \neq 0$  in which the operations  $(D - \sigma I)^{-1}v^{(j)}$  are translated by scalings on each of the subvectors.

---

**Algorithm 2:** Single step of inverse iteration method

---

**Input :**  $D, F, B^T$  and  $B_0$  as defined in (2.13),  $w^{(j)} = \begin{bmatrix} v^{(j)} \\ u^{(j)} \end{bmatrix}$

**Output:**  $w^{(j+1)} = \begin{bmatrix} v^{(j+1)} \\ u^{(j+1)} \end{bmatrix}$

- 1 Compute  $b = u^{(j)} - B^T(D - \sigma I)^{-1}v^{(j)} = u^{(j)} - \sum_{i=1}^m (\sigma_i - \sigma)^{-1} B_i v_i^{(j)}$ ;
- 2 Solve  $S(\sigma)u^{(j+1)} = b$ , with Schur complement matrix  $S(\sigma)$ ;
- 3 Set  $v_i^{(j+1)} = [v_i^{(j)} - u^{(j+1)}]/(\sigma_i - \sigma)$  for  $i = 1, \dots, m$ ;
- 4 **return**  $v^{(j+1)}, u^{(j+1)}$

---

The second part of line 1 of the algorithm executes the operation  $B^T(D - \sigma I)^{-1}$ , exploiting the block structure. Note that the superscripts  $j$  correspond to the iteration number while the subscripts  $i$  correspond to the blocks in the vector  $v^{(j)}$ . Similarly, line 3 unfolds the operation represented by (2.17) into blocks.

*Arnoldi-like schemes and acceleration.* In theory, the above single vector procedure can be applied to generate a certain number of vectors and these can be used to perform a projection step. This would yield a method mathematically equivalent to the Arnoldi procedure applied to the matrix  $\mathcal{A}^{-1}$ . The primary issue with this approach is that it would not be numerically stable. The second issue is that we need to store potentially many vectors, each of length  $mn$  because the Arnoldi procedure requires saving all previous Arnoldi vectors in a given iteration. If  $m$  is large, this will lead to a big demand of memory. Another solution is to use Chebyshev polynomials [38, Sec. 7.4] instead of monomials as in the power method. The vectors generated in this way tend to keep their linear independence longer but we will not consider this approach here.

*Subspace iteration.* We now consider a standard subspace iteration scheme with  $\mathcal{A}^{-1}$ . Suppose we have some initial basis  $W^{(0)}$  with  $\nu$  columns, and apply  $q$  steps of Algorithm 2 to each of its column-vectors. Initially we generate the columns of  $W^{(0)}$  randomly. At the end of the  $q$  steps of the inverse power iteration process we obtain the system  $W^{(q)} = \mathcal{A}^{-q}W^{(0)}$ . This is then orthonormalized to perform a Rayleigh-Ritz procedure applied to the matrix  $\mathcal{A}$ . The algorithm is restarted with  $W^{(0)}$  reset to the most recent Ritz vectors. This results in Algorithm 3 shown below.

---

**Algorithm 3:** Full Subspace Iteration

---

**Input :**  $W^{(0)} \in \mathbb{C}^{(mn+n) \times \nu}$ ;  $q$ ; number of eigenvalues  $k$  (with  $k \leq \nu$ )

**Output:**  $\lambda_1, \dots, \lambda_k, U_k$

```

1 while Convergence not yet reached do
2   for  $j = 0$  to  $q - 1$  do
3     /* Apply Algorithm 2 to each column of  $W^{(j)}$ : */ 
4      $W^{(j+1)} = \mathcal{A}^{-1}W^{(j)}$  ;
5      $W^{(q)} := \text{mgs}(W^{(q)})$ ; /* Orthonormalize  $W^{(q)}$  */
6     /* Apply Rayleigh-Ritz procedure with  $W^{(q)}$  : */
7     Compute:  $\mathcal{A}_p = (W^{(q)})^H \mathcal{A} W^{(q)}$ ;
8     Diagonalize:  $[X, \Lambda] = \text{eig}(\mathcal{A}_p)$ ; /* MATLAB notation */
9     Set:  $W^{(0)} = W^{(q)}X$ ;
10    Test convergence;
11
12 return  $\lambda_1, \dots, \lambda_k$  and eigenvector matrix  $U_k$ 

```

---

Step 3 of the algorithm calls Algorithm 2 which is applied to each column of  $W^{(j)}$ . It can also be restated in block form by using a similar notation as above in which upper-case letters are substituted for lower-case ones:

$$\begin{aligned} U^{(j+1)} &= S^{-1}(U^{(j)} - B^T D^{-1} V^{(j)}), \\ V^{(j+1)} &= D^{-1}(V^{(j)} - F U^{(j+1)}). \end{aligned} \quad \text{for } j = 0, \dots, q - 1.$$

It is common in the subspace iteration algorithm to select a number of columns  $\nu$  that is significantly larger than  $k$  to ensure rapid convergence. For example, it is often recommended to take  $\nu = 2k$ . In step 9 of the algorithm only those  $k$  eigenvalues

obtained from the  $\Lambda$  in step 6 that are closest to the shift  $\sigma$  are returned along with the corresponding eigenvectors which are extracted from the bottom part (' $U$ ' part) of the latest matrix  $W^{(0)}$  calculated in step 7.

It is important to reiterate that none of the steps of Algorithm 3 requires forming matrix  $\mathcal{A}$  explicitly. Steps 3 and 5 take full advantage of the underlying block structure of  $\mathcal{A}$ . However, a disadvantage of Algorithm 3 is that it requires saving a set of basis vectors  $W$  of  $\nu$  vectors each of length  $mn + n$ . All vector operations are performed in a space of dimension  $mn + n$  and when  $m$  is large this can be expensive. A remedy is the reduced approach discussed next which works in a space of dimension  $n$ .

**2.3. Projection method on the reduced system.** This section describes a projection method that works in  $\mathbb{C}^n$ , i.e., it only requires vectors of length  $n$ , the size of the original problem (1.1). Let us consider the surrogate problem (2.5). For now, we assume that we are able to find a subspace  $\mathcal{U}$ , which contains good approximations to eigenvectors of problem (1.1), where  $T(z)$  is of the form (1.5). For the sake of simplicity of the presentation, we will focus on orthogonal projection methods here, noting that generalizations to non-orthogonal methods are straightforward.

Let  $U = [u_1, u_2, \dots, u_\nu]$  be an orthonormal basis of  $\mathcal{U}$ . An approximate eigenvector  $\tilde{u}$  can be expressed in this basis as  $\tilde{u} = Uy$ , with  $y \in \mathbb{C}^\nu$ . Then, a Rayleigh-Ritz procedure applied to (1.1) yields a projected problem:

$$U^H \left( -B_0 + zA_0 + \sum_{i=1}^m \frac{B_i}{z - \sigma_i} \right) Uy = 0. \quad (2.18)$$

This leads to a nonlinear eigenvalue problem in  $\mathbb{C}^\nu$ , namely:

$$\left( -\tilde{B}_0 + z\tilde{A}_0 + \sum_{i=1}^m \frac{\tilde{B}_i}{z - \sigma_i} \right) y = 0, \quad (2.19)$$

in which  $\tilde{A}_0 = U^H A_0 U$ , and  $\tilde{B}_i = U^H B_i U$ , for  $i = 0, 1, \dots, m$ . When  $\nu$  is small this can be handled by solving problem (2.10 – 2.11) directly or by the methods described in the previous sections, even if  $m$  is fairly large.

---

**Algorithm 4:** Reduced Subspace Iteration (no restarts)

---

**Input :** Subspace dimension  $\nu$ ;  $q$ ; Number of eigenvalues  $k$  (with  $k \leq \nu$ )  
**Output:**  $\lambda_1, \dots, \lambda_k, U_k$

- 1 **for**  $j = 1 : \nu$  **do**
- 2    Select  $w = [v; u]$ ; /\* Initially: use random vectors \*/
- 3    Run  $q$  steps of Algorithm 2 starting with  $w$ ;
- 4    If  $w = [v; u]$  is the last iterate, then set  $U(:, j) = u$ ;
- 5 Use  $U$  to compute  $\tilde{B}_0$ ,  $\tilde{A}_0$  and  $\tilde{B}_i$ ,  $i = 1, \dots, m$  from (2.19);
- 6 Solve the reduced eigenvalue problem (2.10) associated with (2.19);
- 7 **return**  $\lambda_1, \dots, \lambda_k$  and eigenvector matrix  $U_k$

---

The question that still remains to be answered is how to obtain a good subspace  $\mathcal{U}$  to perform the projection method. Here, we will rely once more on the surrogate form (2.10 – 2.11) and the vectors obtained from a shift-and-invert approach.

To motivate our approach of obtaining a good basis  $U$ , suppose we wish to perform a single (outer) iteration of Algorithm 3, but that we are only interested in the bottom

part (' $U$ ' part) of the result  $W^{(q)}$  obtained in line 3 of the algorithm. Let a column of  $W^{(0)}$  be of the form  $w^{(0)} = [v^{(0)}; u^{(0)}]$ , where MATLAB notation is used once more and the splitting is relative to the block structure in (2.11). We perform  $q$  steps of the inverse power method for the matrix  $\mathcal{A}^{-1}$  (or  $(\mathcal{A} - \sigma\mathcal{M})^{-1}\mathcal{M}$  in the general case), and denote the  $j$ -th iterate by  $w^{(j)} = [v^{(j)}; u^{(j)}]$ . After a column is processed by  $q$  steps of the power method we discard its top part and add  $u^{(q)}$  to the basis  $U$ . This is done one column at a time and therefore we *only have to keep one vector of length  $mn + n$* . Doing this for all columns of  $U$  constitutes one step of what we call "*reduced subspace iteration*". The resulting technique is summarized in Algorithm 4. To simplify notation, we removed the outer (while) loop that was in Algorithm 3 so, as it is presented, Algorithm 4 is a one-shot method, i.e., it does not include restarts. Restarting can be added and this is discussed next.

In order to restart Algorithm 4, i.e., to add an outer while loop similar to that of Algorithm 3, we need to redefine the vectors  $w$  in line 2. At the very first outer iteration, the vectors  $v$  and  $u$  are just taken as random vectors. In the second iteration and thereafter,  $w = [v; u]$  should ideally be taken to be an approximate eigenvector of (2.10 – 2.11). After the Rayleigh-Ritz projection is performed in line 6, we obtain  $\nu$  approximate eigenpairs for the surrogate problem (2.5). Each of these eigenpairs  $(\lambda, u)$ , yields the bottom ( $U$ -part) of an approximate eigenvector  $w$ , but the corresponding  $v$  vector (top part of  $w$ ) is not available. This is remedied by relying on the relation (2.6), i.e., we define the vector  $v$  by setting each of its  $i$ -th components to be  $v_i = u/(\sigma_i - \lambda)$ .

**3. Theoretical considerations.** Let us consider problem (2.10 – 2.11) under the simplified assumption that  $A_0 = I$ . This is equivalent to having an  $A_0$  that is invertible, since in this case we can multiply equation (1.5) by  $A_0^{-1}$  to reach the desired form in which  $A_0 = I$ . Hence, without loss of generality, we assume  $\mathcal{M} = I$ .

**3.1. Characterization of eigenvalues of  $\mathcal{A}$ .** Now, we would like to examine all the eigenvalues of matrix  $\mathcal{A}$ . For this, we consider the characteristic polynomial of matrix  $\mathcal{A}$ . When  $z$  is different from all the  $\sigma_i$ 's,  $\mathcal{A} - zI$  can be written as:

$$\mathcal{A} - zI = \begin{bmatrix} D - zI & F \\ B^T & B_0 - zI \end{bmatrix}, \quad (3.1)$$

where, referring to (2.11), we see that  $D$  is  $(mn) \times (mn)$ , and  $F$  and  $B$  are both  $(mn) \times n$ . Then, when  $D - zI$  is invertible, the block LU factorization of  $\mathcal{A} - zI$  is:

$$\mathcal{A} - zI = \begin{bmatrix} I & 0 \\ B^T(D - zI)^{-1} & I \end{bmatrix} \begin{bmatrix} D - zI & F \\ 0 & S(z) \end{bmatrix}, \quad (3.2)$$

where  $S(z)$  is the (spectral) Schur complement:

$$S(z) \equiv B_0 - zI - B^T(D - zI)^{-1}F = B_0 - zI + \sum_{i=1}^m \frac{B_i}{\sigma_i - z}. \quad (3.3)$$

Hence, when  $z$  is not a pole, then  $\det(\mathcal{A} - zI) = \det(S(z)) \det(D - zI)$ . Moreover, by comparing equation (2.3) and (3.3) we observe that  $S(z) = -\tilde{T}(z)$ .

Let us assume now that  $z$  is a pole, e.g., without loss of generality let  $z = \sigma_1$ . In this case, we can use a continuity argument. Indeed,  $\det(\mathcal{A} - zI)$  is a continuous

function and therefore we can define  $\det(\mathcal{A} - zI)$  as the limit:

$$\begin{aligned}\det(\mathcal{A} - \sigma_1 I) &= \lim_{z \rightarrow \sigma_1} \det \left[ B_0 - zI + \sum_{i=1}^m \frac{B_i}{\sigma_i - z} \right] \prod_{i=1}^m (\sigma_i - z)^n \\ &= \lim_{z \rightarrow \sigma_1} \det \left[ (\sigma_1 - z)(B_0 - zI) + \sum_{i=1}^m \frac{\sigma_1 - z}{\sigma_i - z} B_i \right] \prod_{i=2}^m (\sigma_i - z)^n \\ &= \det(B_1) \prod_{i=2}^m (\sigma_i - \sigma_1)^n.\end{aligned}$$

Note that a second approach to prove the above relation is to observe that when  $z = \sigma_1$ , then the top left  $n \times n$  block of  $\mathcal{A} - zI$  is a zero block and this can be exploited to expand the determinant.

This result can be generalized to any other  $\sigma_i$ , and therefore we can state the following lemma.

LEMMA 3.1. *The following equality holds :*

$$\det[\mathcal{A} - zI] = \begin{cases} \det(S(z)) \prod_{j=1}^m (\sigma_j - z)^n & \text{if } z \neq \sigma_i \quad i = 1, \dots, m, \\ \det(B_i) \prod_{j \neq i} (\sigma_j - \sigma_i)^n & \text{if } z = \sigma_i. \end{cases} \quad (3.4)$$

Let us denote by  $e_i$  the  $i$ -th canonical basis vector of the vector space  $\mathbb{C}^{m+1}$  and by  $\otimes$  the *Kronecker* product (operator `kron` in MATLAB). The following corollary is an immediate consequence of Lemma 3.1.

COROLLARY 3.2. *If all the matrices  $B_i, i = 0, \dots, m$  are nonsingular, then the eigenvalues of (2.5) are the same as the eigenvalues of matrix  $\mathcal{A}$ . If a matrix  $B_i$  is singular and  $u$  is an associated null vector, then  $\sigma_i$  is an eigenvalue of  $\mathcal{A}$  and  $e_i \otimes u$  is an associated eigenvector.*

Hence, we can ignore any eigenvalue that is equal to one of the  $\sigma_i$ 's when it occurs. The next results will show that as long as the rational approximations of the functions  $f_j : \Omega \rightarrow \mathbb{C}$  are accurate enough, the eigenvalues of  $\tilde{T}(z)$  will be good approximations to all eigenvalues of  $T(z)$  located inside the region  $\Omega$ .

**3.2. Accuracy of computed eigenvalues.** Let  $\Omega_1$  be a region strictly included in the (larger) disk  $\Omega$  such that  $\|f_j(z) - r_j(z)\|_{\Omega_1} < \varepsilon$  where the  $\Omega_1$ -norm is, e.g., the infinity norm in  $\Omega_1$  and  $r_j(z)$  is the rational approximation of function  $f_j(z)$ . In other words, each function  $f_j(z)$  in (1.4) is approximated by a rational function  $r_j(z)$  and this approximation is assumed to be accurate to within an error of  $\varepsilon$  in the region  $\Omega_1$ . Our goal now is to show that each of the eigenvalues inside  $\Omega_1$  is a ‘good’ approximation to an eigenvalue of the original problem (1.1). This can be done by exploiting the corresponding approximate eigenvectors and by considering the residual associated with the approximate eigenpair. The following simple proposition shows a result along these lines.

PROPOSITION 3.3. *Let us assume that  $\|f_j(z) - r_j(z)\|_{\Omega_1} \leq \varepsilon$  for  $j = 1, \dots, p$  and let  $(\tilde{\lambda}, \tilde{u})$  be an exact eigenpair of the surrogate problem (2.5) with  $\tilde{\lambda}$  located inside  $\Omega_1$  and  $\|\tilde{u}\| = 1$  for a certain vector norm  $\|\cdot\|$ . Let  $\mu = \sum_{j=1}^p \|A_j\|$ . Then,*

$$\|T(\tilde{\lambda})\tilde{u}\| \leq \mu\varepsilon.$$

*Proof.* The approximate problem (2.5) is obtained by replacing  $T(z)$  in (1.5) by:

$$\tilde{T}(z) = -B_0 + zA_0 + r_1(z)A_1 + \dots + r_p(z)A_p. \quad (3.5)$$

Since  $(\tilde{\lambda}, \tilde{u})$  is an eigenpair of problem (2.5),  $\tilde{T}(\tilde{\lambda})\tilde{u} = 0$ , which implies

$$[-B_0 + \tilde{\lambda}A_0 + r_1(\tilde{\lambda})A_1 + \dots + r_p(\tilde{\lambda})A_p]\tilde{u} = 0.$$

Setting  $r_j(\tilde{\lambda}) - f_j(\tilde{\lambda}) = \eta_j(\tilde{\lambda})$  and substituting this into above equation gives

$$\begin{aligned} & [-B_0 + \tilde{\lambda}A_0 + \sum_{j=1}^p (f_j(\tilde{\lambda}) - \eta_j(\tilde{\lambda}))A_j]\tilde{u} = 0, \\ & [-B_0 + \tilde{\lambda}A_0 + \sum_{j=1}^p f_j(\tilde{\lambda})A_j]\tilde{u} = \left[ \sum_{j=1}^p \eta_j(\tilde{\lambda})A_j \right] \tilde{u}, \end{aligned}$$

and thus  $T(\tilde{\lambda})\tilde{u} = \left[ \sum_{j=1}^p \eta_j(\tilde{\lambda})A_j \right] \tilde{u}$ . Taking norms on both sides and recalling that  $\|f_j(z) - r_j(z)\|_{\Omega_1} \leq \varepsilon$  yields:  $\|T(\tilde{\lambda})\tilde{u}\| = \left\| \sum_{j=1}^p \eta_j(\tilde{\lambda})A_j \tilde{u} \right\| \leq \mu\varepsilon$ , which is the desired result.  $\square$

Proposition 3.3 implies that any eigenpair of problem (2.5) is an approximate eigenpair of the original problem provided that each function  $f_j(z)$  is well approximated by a rational function  $r_j(z)$  in  $\Omega_1$  and that the eigenvalue  $\tilde{\lambda}$  is inside  $\Omega_1$ . By a backward argument the opposite is also true.

**PROPOSITION 3.4.** *Let us assume that  $\|f_j(z) - r_j(z)\|_{\Omega_1} \leq \varepsilon$  for  $j = 1, \dots, p$  and let  $(\lambda, u)$  be an exact eigenpair for  $T(z)$  with  $\lambda$  located inside  $\Omega_1$  and  $\|u\| = 1$ . Then,  $(\lambda, u)$  is an approximate eigenpair of the problem (2.5), i.e.,*

$$\|\tilde{T}(\lambda)u\| \leq \mu\varepsilon,$$

where  $\mu$  is defined as in Proposition 3.3.

*Proof.* The proof is essentially identical to that of Proposition 3.3.  $\square$

These two results show that for  $\varepsilon$  small enough, we should be able to find approximations to all eigenvalues of the exact problem located in  $\Omega_1$  (and only these) by solving (2.5), except for cases with very bad ill-conditioning.

**3.3. Conditioning of a simple eigenvalue.** For the reason stated above, it is of particular importance to examine the condition number of an eigenvalue of the extended problem (2.10 – 2.11). As before, we assume that  $A_0 = I$ . Let us consider a simple eigenvalue  $\lambda$  of the matrix  $\mathcal{A}$ . Its right eigenvector is a vector  $w$  of the form shown in (2.9) with  $v_i = u/(\sigma_i - \lambda)$  defined in (2.6). As seen earlier – equation (2.5) – the vector  $u$  is an eigenvector of  $S(\lambda)$ , i.e., we have  $S(\lambda)u = 0$ .

The left eigenvector is a vector  $s$  that satisfies  $\mathcal{A}^H s = \bar{\lambda} s$ . Similarly to  $w$ , it consists of block components  $h_1, \dots, h_m$ , and  $y$ . The equation  $(\mathcal{A}^H - \bar{\lambda}I)s = 0$  yields the relations:

$$(\bar{\sigma}_i - \bar{\lambda})h_i + B_i^H y = 0 \quad \Rightarrow \quad h_i = \frac{1}{\bar{\lambda} - \bar{\sigma}_i} B_i^H y, \quad i = 1, \dots, m$$

and

$$-\sum_{i=1}^m h_i + (B_0^H - \bar{\lambda}I)y = 0 \quad \Rightarrow \quad S(\lambda)^H y = 0.$$

Thus, the right and the left eigenvectors of  $\mathcal{A}$  are defined in terms of the right and the left eigenvectors  $u$  and  $y$  of  $S(\lambda)$ .

As is well-known the condition number of a single eigenvalue  $\lambda$  is the inverse of the cosine of the acute angle between the left and the right eigenvectors. Before considering the inner product  $(w, s)$ , we point out that the derivative of  $S(z)$  is:

$$S'(z) = -I + \sum_{i=1}^m \frac{B_i}{(z - \sigma_i)^2}. \quad (3.6)$$

Consider now the inner product  $s^H w$ :

$$s^H w = y^H u + \sum_{i=1}^m h_i^H v_i = y^H u - \sum_{i=1}^m \frac{y^H B_i u}{(\lambda - \sigma_i)^2} = -y^H S'(\lambda) u.$$

Finally, we need to calculate the norms of  $s$  and  $w$ . For  $w$  we have

$$\|w\|_2^2 = \|u\|^2 + \sum_{i=1}^m \frac{\|u\|_2^2}{|\lambda - \sigma_i|^2} = \|u\|^2 \left[ 1 + \frac{1}{|\lambda - \sigma_i|^2} \right],$$

while for  $s$ :

$$\|s\|_2^2 = \|y\|^2 + \sum_{i=1}^m \frac{\|B_i y\|_2^2}{|\lambda - \sigma_i|^2} = \|y\|^2 \left[ 1 + \sum_{i=1}^m \frac{\|B_i y\|_2^2}{\|y\|_2^2 |\lambda - \sigma_i|^2} \right].$$

Assuming that the vectors  $u$  and  $y$  are of norm one leads to the following proposition which establishes an expression for the desired condition number.

**PROPOSITION 3.5.** *Let  $\lambda$  be a simple eigenvalue of (2.11), and  $u, y$  the corresponding unit norm right and left eigenvectors (respectively) of  $S(\lambda)$ . Then the condition number of  $\lambda$  as an eigenvalue of (2.10 – 2.11) is given by*

$$\kappa(\lambda) = \frac{\alpha_u \alpha_y}{|(S'(\lambda)u, y)|}, \quad (3.7)$$

where

$$\alpha_u = \sqrt{1 + \sum_{i=1}^m \frac{1}{|\lambda - \sigma_i|^2}} \quad \text{and} \quad \alpha_y = \sqrt{1 + \sum_{i=1}^m \frac{\|B_i y\|_2^2}{|\lambda - \sigma_i|^2}}. \quad (3.8)$$

The coefficients  $\alpha_u, \alpha_y$  will remain bounded as long as  $\lambda$  is far away from any of the poles. Note in particular that the terms  $\|B_i y\|_2$  can be bounded by the constant  $\beta = \max_i \|B_i\|_2$ . On the other hand nothing will prevent the denominator in (3.7) from being close to zero. The condition number can be easily gauged to determine if this is the case. Note that  $y^H S'(\lambda) u$  is inexpensive to compute once the eigenvectors  $u$  and  $y$  are available.

**3.4. The halo of extraneous eigenvalues.** In all our experiments we observed that the eigenvalues of the problem (2.10 – 2.11) that are not eigenvalues of the original nonlinear problem (1.5) tend to congregate into a ‘halo’ around the contour  $\Gamma$  used for the Cauchy integration.

It is possible to explain this phenomenon. First note that the basis of the method under consideration is to approximate the original nonlinear matrix function  $T(z)$  in (1.5) by the rational function:

$$\tilde{T}(z) = -B_0 + zA_0 + r_1(z)A_1 + \dots + r_p(z)A_p, \quad (3.9)$$

where each  $r_j(z)$  is an approximation of  $f_j(z)$ .

Consider the situation when  $z$  is outside the domain used to obtain the Cauchy integral, far from the contour. Assuming that  $m$  is large enough, then each  $r_j(z)$  will be close to zero. Hence, any eigenvalue  $\lambda$  of  $\tilde{T}(z)$  that is outside the contour and not too close to it should be just an eigenvalue of the generalized problem  $(B_0 - \lambda A_0)u = 0$ . In other words, it should be close to an eigenvalue of the linear part of  $T(z)$ .

Let us now consider the opposite case of an eigenvalue of  $\tilde{T}(z)$  that is inside the contour but also not too close to it. Our earlier results show that in this case we should only find eigenvalues of the original problem (1.5) and no other eigenvalues.

For an eigenvalue to be *extraneous*, i.e., in the spectrum of (2.10 – 2.11) but not of (1.5), it must therefore *either be (close to) an eigenvalue of the linear part of  $T(z)$ , or located (close to) the contour*.

Although this argument is based on a simple model, it provides a picture that is remarkably close to what is observed in practice. Next we present an illustration using a small quadratic eigenvalue problem. Quadratic eigenvalue problems can be handled more efficiently by standard linearization than by the method presented in this paper. However, they can be useful for the purpose of validation because their eigenvalues are readily available. Consider the problem

$$(-B_0 + \lambda A_0 + \lambda^2 A_2)u = 0, \quad (3.10)$$

where the matrices  $B_0, A_0, A_2$  are generated by the following three MATLAB lines of code with  $n = 4$ :

```
B0 = -2*eye(n)+diag(ones(n-1,1),1)+diag(ones(n-1,1),-1) ;
A0 = eye(n);
A2 = 0.5*(n*eye(n)-eye(n,1)*ones(1,n)-ones(n,1)*eye(1,n));
```

The eigenvalues are all located inside a rectangle with bottom-left and top-right corners  $(-1, -1.5i)$ ,  $(0, 1.5i)$  which we use as the integration contour.

Gauss-Legendre quadrature formulas are invoked on each side of the rectangle with a number of points selected to be proportional to the side length. The left side of Figure 3.1 shows the 8 eigenvalues of the original problem (1.5) as well as the 4 eigenvalues of the pencil  $(B_0, A_0)$ . Three of these eigenvalues are located outside the contour and one inside. The right part of Figure 3.1 and the two plots in Figure 3.2 show the eigenvalues of problem (2.10 – 2.11) when the number of contour points is  $m = 20, 32, 60$ , respectively. When  $m = 20$  the approximations are still rough. However, the pattern mentioned above begins to unravel: the eigenvalues of (3.10) located inside the contour are more or less approximated, and those eigenvalues of  $(B_0, A_0)$  that are outside are starting to be neared by pluses. Observe that the eigenvalue of  $(B_0, A_0)$  that is near  $-1.5$  is approximated by two eigenvalues of  $\mathcal{A}$ . In contrast, the one near  $-0.5$  (inside the contour) is not approximated as predicted by the theory. As  $m$  increases this picture is confirmed: (1) all the eigenvalues of (3.10) inside the contour are well approximated, (2) all the eigenvalues of  $(B_0, A_0)$  outside the contour are well approximated by eigenvalues of  $\mathcal{A}$ , and (3) the eigenvalue of  $(B_0, A_0)$  inside the contour is essentially ‘ignored’. In addition, the halo of eigenvalues around

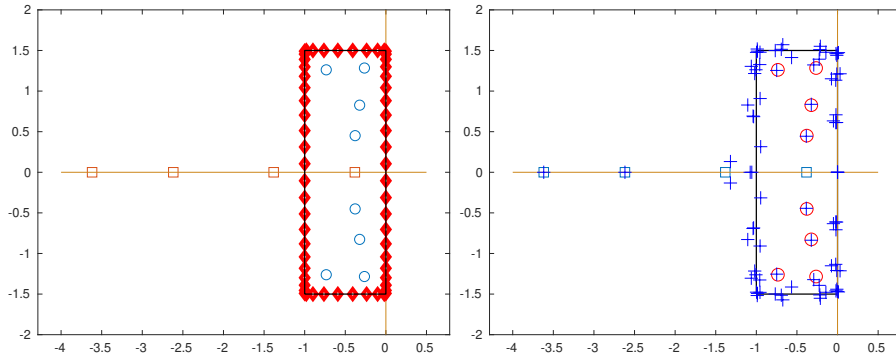


FIG. 3.1. Left: The 8 eigenvalues of the original problem (3.10) (circle); the 4 eigenvalues of the linear part (square); contour and quadrature points along it. Right: Eigenvalues computed with  $m = 20$  quadrature points (plus) along with contour, original eigenvalues (circle), and eigenvalues of linear part (square).

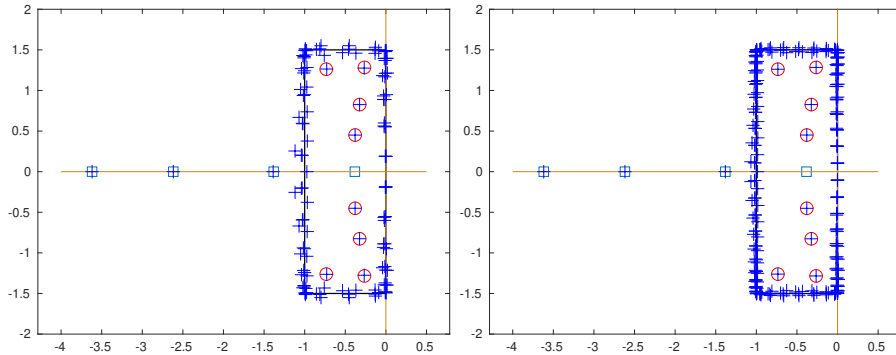


FIG. 3.2. Same information as in the right part of Figure 3.1 using a total of  $m = 32$  quadrature points (left) and  $m = 60$  quadrature points (right).

the contour becomes quite close to the contour itself. This small example provides a good illustration of the general behavior that we observe in our experiments.

**4. Numerical Experiments.** All the numerical experiments presented in this section were performed with MATLAB R2018a. We will illustrate the behavior of Algorithms 1, 3 and 4 on several nonlinear eigenvalue problems discussed in [8, 35, 21]. All the examples considered come in the form given in (1.5). For most of the examples, the contour  $\Gamma$  is either circular or rectangular and we seek the eigenvalues closest to the center of  $\Gamma$ . For Algorithms 1 and 4, the shift  $\sigma$  is selected to be the center of the region enclosed by the contour  $\Gamma$ .

In the case of a circular contour, the  $m$  quadrature nodes and weights used to perform the numerical integration to approximate the functions  $f_j$  inside the contour  $\Gamma$  were generated using the Gauss-Legendre quadrature rule. To choose a suitable  $m$ , we take two circles  $\Omega_1$  and  $\Omega$  with the same center and  $\Omega_1 \subset \Omega$ . Then,  $m$  is increased until the accuracy of the resulting rational approximation is high enough inside  $\Omega_1$ . Note that we need to avoid a region near the outer circle not only because of the poles, but also because the approximations of the  $f_j$ 's will tend to be poor in this region. To illustrate the effectiveness of the proposed approaches, we compare the eigenvalues obtained by each algorithm with the ones obtained by Beyn's method [8]

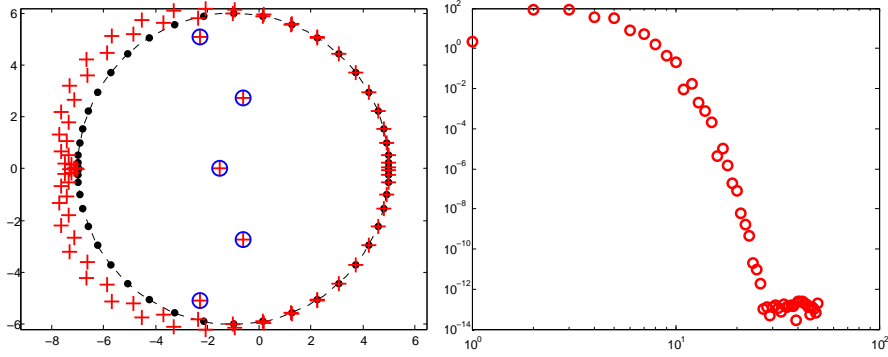


FIG. 4.1. Left: Eigenvalues of (4.1) inside a circle of radius  $r = 6$  centered at  $c = -1$  obtained by solving the eigenvalue problem (2.10) (plus) using  $m = 50$  quadrature nodes (point) and by Beyn's method (circle) using 150 quadrature nodes. Right: The errors  $e_m$  of the rational approximation of  $e^{-z}$  versus the number of quadrature nodes  $m$ .

or/and via a corresponding linearization.

**Example 1.** Consider the following example discussed in [30, Sec. 2.4.2] and [21, Example 13],

$$T(z) = -B_0 + zI + e^{-z\tau}A_1, \quad (4.1)$$

with  $B_0 = \begin{pmatrix} -5 & 1 \\ 2 & -6 \end{pmatrix}$ ,  $A_1 = -\begin{pmatrix} -2 & 1 \\ 4 & -1 \end{pmatrix}$  and  $\tau = 1$ . The nonlinear eigenvalue problem (4.1) is the characteristic equation of a delay system  $x'(t) = -B_0x(t) + A_1x(t - \tau)$ . For the purpose of a comparison with the results from [8, Example 5.5], we calculate all eigenvalues enclosed by a circle centered at  $c = -1$  with radius  $r = 6$ . Referring to Proposition 3.3 we first check which values of  $m$  will provide a good rational approximation  $r_m(z)$  of  $f(z) = e^{-z}$ . The right part of Figure 4.1 shows the errors  $e_m = \|f(z) - r_m(z)\|_\infty$  (evaluated on a finely discretized version of  $\Omega_1$ ) versus the number of quadrature nodes  $m$ . Notice that the accuracy of the rational approximation of  $f(z)$  inside the considered contour is good enough for  $m = 50$ . We can therefore solve the eigenvalue problem (2.10) associated with the approximate problem (2.5) with  $m = 50$  Gauss-Legendre quadrature nodes. The left part of Figure 4.1 compares the eigenvalues computed by Algorithm 1 and those computed by Beyn's method using the same contour. Note that the number of quadrature nodes for Beyn's method necessary to get the five eigenvalues inside the circle is 150.

In order to check the conclusions of Proposition 3.3, we compute again all the eigenvalues of the generalized eigenvalue problem (2.10) associated with the approximate problem (2.5) inside a circle  $\Omega$  centered at  $c = -1$  with radius  $r = 6$ , using  $m = 100$  quadrature nodes. These eigenvalues are shown on the left side of Figure 4.2. Let  $\Omega_1$  be a disk with the same center as  $\Omega$  and with radius  $r_1 = r/2$ . Let  $\lambda_1$  be the closest eigenvalue to  $c$  located in  $\Omega_1$  and  $u_1$  be the corresponding eigenvector. Recall that  $u_1$  is taken from the last  $n$  entries of the eigenvector corresponding to the eigenvalue  $\lambda_1$  of (2.10). Let  $\mu$  be the constant from Proposition 3.3 and  $r_m(z)$  the rational approximation of the function  $f(z) = e^{-z}$ . The right-hand side of Figure 4.2 compares the residuals  $\|T(\lambda_1)u_1\|_\infty$  with the errors  $e_m = \mu\|f(z) - r_m(z)\|_\infty$  when the number of quadrature nodes  $m$  varies.

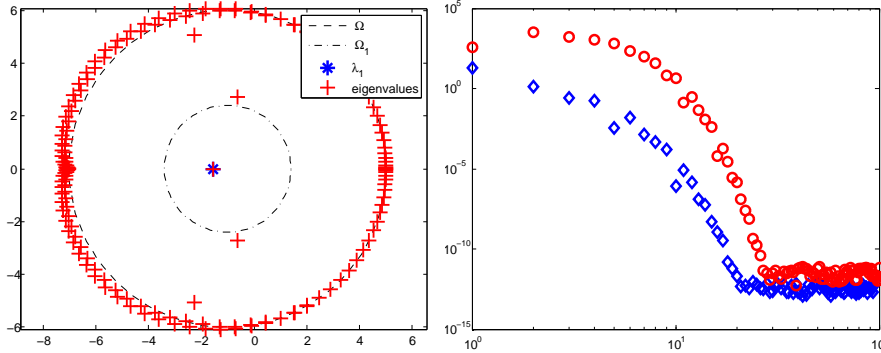


FIG. 4.2. Left: All eigenvalues of (4.1) (plus) computed via (2.10). Right: Residuals  $\|T(\lambda_1)u_1\|_\infty$  (diamond) and errors  $e_m$  (circle) versus the number of quadrature nodes  $m$ .

**Example 2.** In this experiment, we consider the same nonlinear eigenvalue problem as in Example 1 with a different search contour. The location of the eigenvalues in Example 1 suggests that it should be more effective to consider a rectangular contour instead of a disk. An advantage of rectangular regions is that they are easier to subdivide into smaller rectangular regions than disks. For example, we can split a rectangle in the complex plane into different sub-rectangles and then apply Algorithm 1 or Algorithm 4 in each sub-rectangle. A side benefit of this approach is the added parallelism since each sub-rectangle can be processed independently. Finally, this divide-and-conquer approach also allows to take advantage of the trade-off between using smaller regions which require fewer poles versus larger regions which will yield more eigenvalues at once at the cost of using more poles.

If  $c_1, c_2, c_3, c_4$  are the four corners of the rectangle, listed counter clock-wise with  $c_1$  being the top-left corner, the integration starts at  $c_1$ , and is performed counter-clockwise using Gauss-Legendre quadrature on each side. To solve the nonlinear eigenvalue problem (4.1), we consider the rectangle defined by the two opposite corners at  $c_2 = -3 - 6i$  and  $c_4 = 1 + 6i$ , and we solve the eigenvalue problem (2.10) directly, using  $m = 40$  quadrature points. The left part of Figure 4.3 shows that all eigenvalues are well approximated inside the rectangle. To illustrate the behavior of the rational approximation method for the nonlinear eigenvalue problem near the nodes, we consider a smaller rectangle defined by  $c_2 = -2.5 - 6i$  and  $c_4 = -0.2 + 6i$ . As we can clearly see on the right-hand side of Figure 4.3, eigenvalues near the quadrature nodes are not well approximated. This is a consequence of the poor rational approximation of the function  $f(z) = e^{-z}$  near the quadrature nodes. Good eigenvalue approximations can be computed by increasing the number of quadrature nodes on each side. This is illustrated in Figure 4.4 in which  $m = 50$  quadrature nodes are considered.

**Example 3.** As our next example, we consider the following nonlinear eigenvalue problem, see [43, 21],

$$T(z) = B_0 + zA_0 + \frac{1}{1-z}e_n e_n^T, \quad (4.2)$$

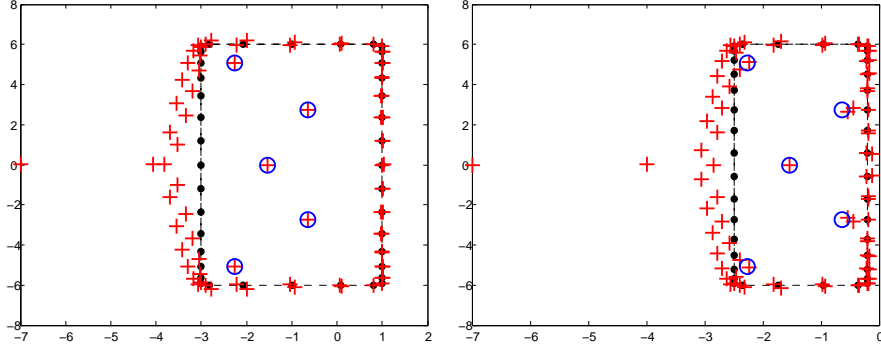


FIG. 4.3. Left: Eigenvalues of (4.1) obtained by solving the eigenvalue problem (2.10) inside a rectangle defined by  $c_2 = -3 - 6i$  and  $c_4 = 1 + 6i$  with  $m = 40$  quadrature nodes (plus) obtained by Beyn's method (circle) Right: Eigenvalues of (4.1) obtained by solving the eigenvalue problem (2.10) inside a rectangle defined by  $c_2 = -2.5 - 6i$  and  $c_4 = -0.2 + 6i$  with  $m = 40$  quadrature nodes (plus) obtained by Beyn's method (circle).

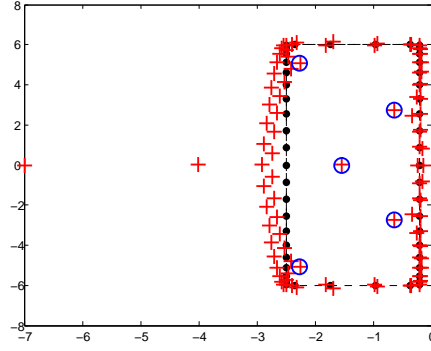


FIG. 4.4. Eigenvalues of (4.1) obtained by solving the eigenvalue problem (2.10) inside a rectangle defined by  $c_2 = -2.5 - 6i$  and  $c_4 = -0.2 + 6i$  with  $m = 50$  quadrature nodes (plus) and by Beyn's method (circle).

with

$$B_0 = n \begin{pmatrix} 2 & -1 & & \\ -1 & \ddots & \ddots & \\ & \ddots & 2 & -1 \\ & & -1 & 1 \end{pmatrix}, \quad A_0 = -\frac{1}{6n} \begin{pmatrix} 4 & 1 & & \\ 1 & \ddots & \ddots & \\ & \ddots & 4 & 1 \\ 1 & 2 & & \end{pmatrix},$$

resulting from the finite element discretization of the nonlinear boundary eigenvalue problem

$$-u''(x) = \lambda u(x), 0 \leq x \leq 1, \quad u(0) = u'(1) + \frac{\lambda}{\lambda - 1} u(1) = 0. \quad (4.3)$$

To compare our results with those obtained by Beyn's method [8, Example 4.11], we consider the case when  $n = 100$  and compute five eigenvalues enclosed by a circle centered at  $c = 150$  with radius  $r = 150$ . We first determine the number of quadrature nodes  $m$  needed to get a good rational approximation of the function  $f(z) = \frac{1}{1-z}$

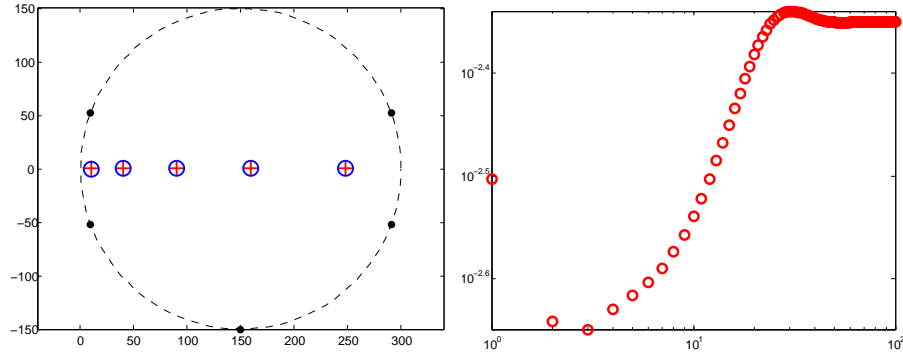


FIG. 4.5. Left: Eigenvalues of (4.2) inside a circle of radius  $r = 150$  centered at  $c = 150$  obtained by Algorithm 1 (plus) and by Beyn's method (circle). Right: The errors  $e_m$  of the rational approximation of  $f(z) = \frac{1}{1-z}$  versus the number of quadrature nodes  $m$ .

inside the considered circular contour  $\Gamma$ . The right part of Figure 4.5 shows the approximation error for the rational approximation of  $f(z)$  versus  $m$ .

Because  $f(z)$  is itself a rational function a high enough accuracy is obtained for a small value of  $m$ , namely  $m = 6$ . Therefore, we apply Algorithm 1 with  $m = 6$  and  $\sigma = c$  to get the approximate eigenvalues inside the circle. The computed eigenvalues are shown on the left of Figure 4.5. These results are directly compared with the ones obtained by Beyn's method using 50 quadrature nodes.

Note that the function  $f(z)$  is already given in a rational form and so we can solve (4.2) by considering the same linearization as the one invoked in Section 2:

$$\begin{bmatrix} I & -I \\ e_n e_n^T & B_0 \end{bmatrix} \begin{bmatrix} \frac{u}{1-z} \\ u \end{bmatrix} = z \begin{bmatrix} I & 0 \\ 0 & -A_0 \end{bmatrix} \begin{bmatrix} \frac{u}{1-z} \\ u \end{bmatrix}. \quad (4.4)$$

Figure 4.6 compares the eigenvalues obtained by solving (4.4) and the ones computed by Algorithm 1.

Alternatively, we can solve problem (4.2) directly using Algorithm 4 without restarts. Let  $w_i = [v_i; u_i]$ ,  $i = 1, \dots, \nu$  be a set of  $\nu$  random vectors of size  $N = (m+1)n$ , where  $v_i \in \mathbb{R}^{mn}$  and  $u_i \in \mathbb{R}^n$ . For this experiment, we choose  $\nu = 7$  and we apply  $q = 5$  steps of Algorithm 2 on each  $w_i$ . We orthogonalize the resulted vectors  $U = [u_1, u_2, \dots, u_\nu]$  to obtain a good subspace to perform the projection method introduced in Algorithm 4. We recall that using Algorithm 4 allows to work with vectors of size  $n$  only, while Algorithm 1 requires storing vectors of length  $N = (m+1)n$ . As for Algorithm 1, we choose  $m = 6$  and we use Algorithm 4 to compute the eigenvalues enclosed by the same circular contour. As can be seen on the left of Figure 4.6, the eigenvalues obtained by Algorithm 4 are in good agreement with those obtained by Algorithm 1 and by Beyn's method.

**Example 4: Hadeler problem.** As an example of a general nonlinear eigenvalue problem, we consider the *Hadeler problem* [17, 35, 6]:

$$T(\lambda) = (e^\lambda - 1)B_1 + \lambda^2 B_2 - B_0, \quad (4.5)$$

with the coefficient matrices

$$B_0 = b_0 I, \quad B_1 = (b_{jk}^{(1)}), \quad B_2 = (b_{jk}^{(2)}), \quad (4.6)$$

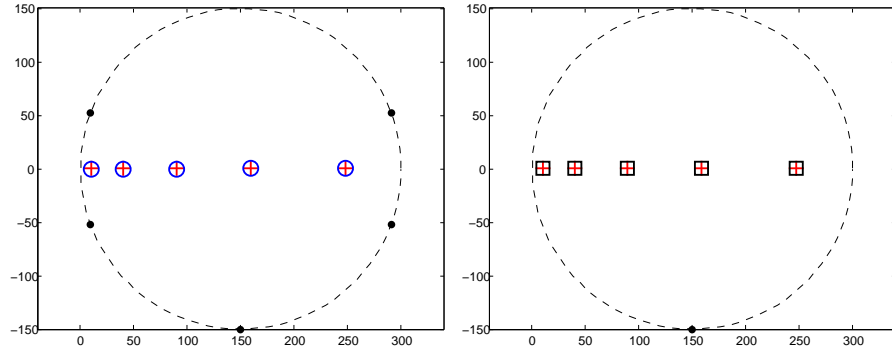


FIG. 4.6. Left: Eigenvalues of (4.2) inside a circle of radius  $r = 150$  centered at  $c = 150$  obtained by Algorithm 4 (plus) and by Beyn's method (circle). Right: Eigenvalues of (4.2) inside a circle of radius  $r = 150$  centered at  $c = 150$  obtained by Algorithm 1 (plus) and by linearization (4.4) (square).

$$b_{jk}^{(1)} = (n + 1 - \max(j, k))jk, \quad b_{jk}^{(2)} = n\delta_{jk} + 1/(j + k), \quad (4.7)$$

of dimension  $n$  and a parameter  $b_0 = 100$  (following reference [35]). For our experiments we choose  $n = 200$ .

We refer the reader to the above articles for details on this problem. The eigenvalues of (4.5) are real with  $n$  of them being negative and  $n$  positive. The eigenvalues become better spaced as we move away from the origin and the smallest one is close to  $-48$ . We compute the eigenvalues inside a circle centered at  $c = -30$  with radius  $r = 10$ . Using  $m = 50$  Gauss-Legendre quadrature nodes, 12 eigenvalues of (4.5) were computed using Algorithm 1. These results are compared with the approximations obtained by Beyn's method [8], see Figure 4.7.

We repeat the same experiment using the reduced subspace iteration given by Algorithm 4 with restarts. We first start with  $\nu = 24$  random vectors, where  $\nu$  is the dimension of the subspace in Algorithm 4 and then apply  $q = 10$  steps of Algorithm 2 on each of these vectors separately to obtain a block of  $\nu$  vectors each one of size  $n$ . Note that these vectors are the resulting bottom parts of the final iterates of Algorithm 2. These  $\nu$  bottom parts are orthogonalized to obtain an orthonormal basis  $U$  used to perform Rayleigh-Ritz projection that leads to a nonlinear eigenvalue problem in  $\mathbb{C}^\nu$  of the form (2.19). We then solve this reduced (nonlinear) eigenvalue problem (2.19) by computing the eigenvalues and vectors of the expanded problem (2.10 – 2.11) that are obtained from it. Note that this problem is now of size  $(m + 1)\nu$ . Before each restart of Algorithm 4, we select  $\nu$  approximate eigenpairs whose eigenvalues are inside the contour. The initial vectors  $w$  selected in line 2 of Algorithm 4 with restarting are of the form  $w = [v; u]$  where the components  $v_i$  of  $v$  satisfy  $v_i = u/(\sigma_i - \lambda)$ . Here  $(\lambda, u)$  is one of the  $\nu$  approximate eigenpairs computed from the previous outer iteration. At the very first outer iteration  $v$  and  $u$  are random vectors. The resulting bottom parts of the final iterates are used to form the block  $U$  of Algorithm 4 with restarting. The columns of  $U$  are orthonormalized before applying the Rayleigh-Ritz procedure in lines 5–6. The outer iteration of Algorithm 4 is stopped when

$$\sum_{i=1}^k \|\tilde{T}(\lambda_i)u_i\| \leq tol * \sum_{i=1}^k \left( \|B_0\| + |\lambda_i| \|A_0\| + \sum_{j=1}^p |r_j(\lambda_i)| \|A_j\| \right). \quad (4.8)$$

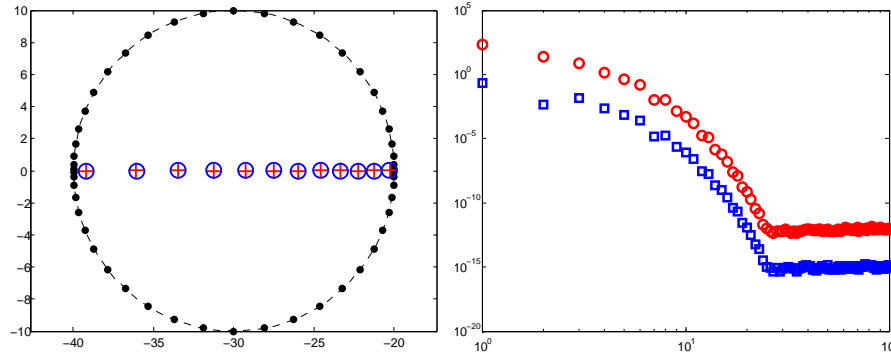


FIG. 4.7. Left: Eigenvalues of (4.5) inside a circle of radius  $r = 10$  and center  $c = -30$  obtained by Algorithm 1 (plus), by Beyn's method (circle). Right: The residual norm of the rational approximation of  $e^z - 1$  (square) and  $z^2$  (circle) versus the number of quadrature nodes  $m$ .

where  $\|\cdot\|$  stands for the 2-norm. We run as many outer iterations as needed to achieve convergence with a tolerance of  $tol = 10^{-10}$ . Algorithm 4 computed the same 12 eigenvalues of (4.5) as those obtained by Algorithm 1, requiring 13 outer iterations to satisfy the above stopping criterion. To verify that the computed eigenpairs are good approximations to the original problem, we computed the residual norm sum scaled similarly to (4.8) and found that for problem (4.5) we have

$$\sum_{i=1}^k \frac{\|T(\lambda_i)u_i\|}{\gamma} \approx 9.28 \times 10^{-14},$$

at the end of Algorithm 4, where  $\gamma = \sum_{i=1}^k (\|B_0\| + |\lambda_i| \|A_0\| + \sum_{j=1}^p |f_j(\lambda_i)| \|A_j\|)$ .

Another way to extract those 12 eigenvalues of interest is to resort to the rational approximation using the Cauchy integral formula inside an elliptic contour. We consider an ellipse centered at  $c = -30$  with semi-major axis  $r_x = 10$  and semi-minor axis  $r_y = 1$  on the  $x$ -axis and  $y$ -axis, respectively. We can use Algorithm 1 with  $m = 8$  and  $\sigma = c$  and perform as many steps as needed to extract all 12 real eigenvalues inside the elliptic contour. In Figure 4.9, we present the eigenvalues computed by Algorithm 1 and by Beyn's integral method using the same elliptic contour. For Beyn's method 50 trapezoidal quadrature nodes are necessary to get those 12 eigenvalues.

**Example 5: Butterfly Problem.** To illustrate the behavior of rational approximation methods when using a contour centered at an arbitrary point in the complex plane, we present a few results with the *butterfly problem* (so called because of the distribution of its eigenvalues in the complex plane) available from the NLEVP collection [6]. This is a quartic eigenvalue problem of the form

$$T(\lambda) = A_0 + \lambda A_1 + \lambda^2 A_2 + \lambda^3 A_3 + \lambda^4 A_4, \quad (4.9)$$

where  $A_0, A_1, \dots, A_4$  are structured matrices of size  $n = 64$ . The 256 eigenvalues of this problem are shown on the left side of Figure 4.10. A detailed description of this example can be found in [28]. We use Algorithm 1 with  $m = 50$  quadrature nodes to compute the eigenvalues enclosed by a circle centered at  $c = 1 + 1i$  with radius  $r = 0.5$ . We compare approximations of 13 computed eigenvalues with those determined by the linearization of problem (4.9) and by application of Beyn's method. The right part of

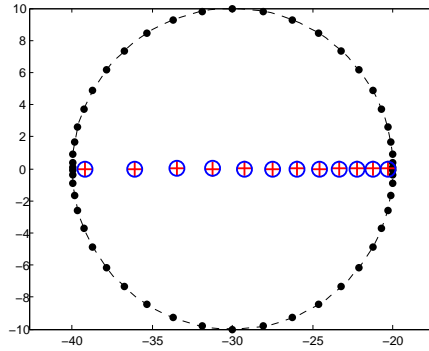


FIG. 4.8. Eigenvalues of (4.5) inside a circle of radius  $r = 10$  and center  $c = -30$  obtained by Algorithm 4 (plus) and by Beyn's method (circle).

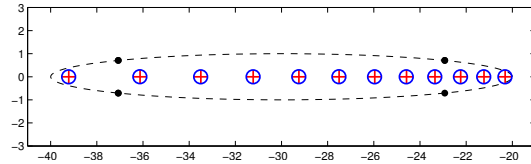


FIG. 4.9. Eigenvalues of (4.5) inside an ellipse centered at  $c = -30$  and with semi-major axis  $r_x = 10$  and semi-minor axis  $r_y = 1$  obtained by Algorithm 1 (plus) and by Beyn's method (circle).

Figure 4.10 summarizes our findings. Alternatively, we can use a rectangular contour as described already in Example 2. Figure 4.11 shows approximations of 17 eigenvalues enclosed by the rectangular contour defined by the corners  $c_2 = (0.55, 0.48)$  and  $c_4 = (1.2, 1.3)$  obtained using Algorithm 1 with  $m = 90$  quadrature nodes and direct linearization.

**5. Concluding remarks.** An appealing feature of the general approach proposed in this paper for solving nonlinear eigenvalue problems is its simplicity. A general nonlinear problem is approximated by a rational eigenvalue problem which is then linearized. The resulting linear problem provides the basis for developing a number of methods and three of these, among possibly many others, were discussed in this paper. The theory allows us to exactly predict which eigenvalues of the original problem are well approximated and it also tells us that no eigenvalues in the region will be missed. Another attribute of the method is its flexibility. It is possible to compute all eigenvalues in a union of small regions each requiring a small number of poles, or to use one single large region to compute many eigenvalues but now with a large number of poles. Finally, the method has a good potential for solving realistic large sparse nonlinear eigenvalue problems such as those mentioned in the introduction. In this regard, we note that *only one factorization is required* namely that of  $S(\sigma)$  where  $\sigma$  is the shift in the shift-and-invert procedure. In many applications the patterns of the matrices  $A_j$  are not too different from one another and so  $S(\sigma)$ , which is itself a combination of the  $A_j$ 's, will remain sparse.

## REFERENCES

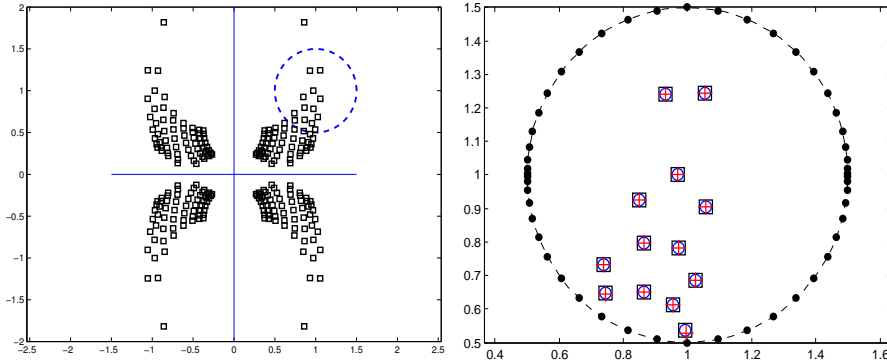


FIG. 4.10. Left: All 256 eigenvalues of butterfly example 4 (square) obtained by linearization. Circle contour centered at  $c = 1 + 1i$  with radius  $r = 0.5$  (dashed). Right: Eigenvalues of butterfly example (4.9) inside a circle of radius  $r = 0.5$  centered at  $c = 1 + 1i$  obtained by Algorithm 1 (plus) with  $m = 50$ , by linearization (square) and by Beyn's method (circle).

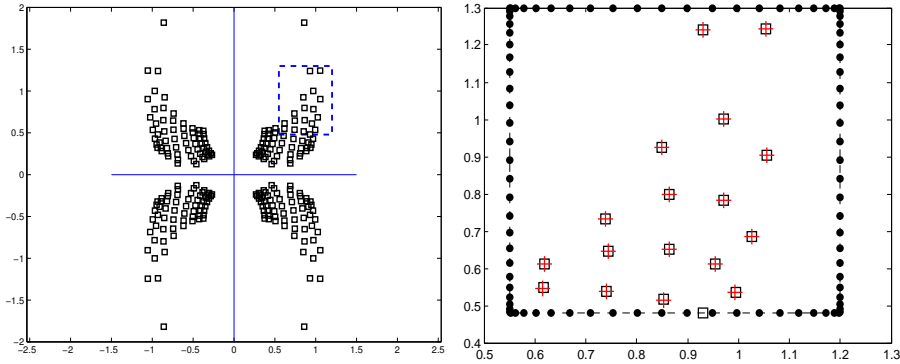


FIG. 4.11. Left: All 256 eigenvalues of butterfly example 4 (square) obtained by linearization. Rectangular contour centered at  $0.875 + 0.89i$  with corners  $(0.55, 1.3)$ ,  $(0.55, 0.48)$ ,  $(1.2, 0.48)$  and  $(1.2, 1.3)$  (dashed). Right: Eigenvalues of butterfly example (4.9) inside a rectangular contour obtained by Algorithm 1 (plus) with  $m = 90$  and by linearization.

- [1] J. ASAKURA, T. SAKURAI, H. TADANO, T. IKEGAMI, AND K. KIMURA, *A numerical method for nonlinear eigenvalue problems using contour integrals*, JSIAM Lett., 1 (2009), pp. 52–55.
- [2] J. ASAKURA, T., SAKURAI, H. TADANO, T. IKEGAMI, AND K. KIMURA, *A numerical method for polynomial eigenvalue problems using contour integral*, Jpn. J. Ind. Appl. Math., 27 (2010), pp. 73–90.
- [3] Z. BAI AND Y. SU, *SOAR: a second-order Arnoldi method for the solution of the quadratic eigenvalue problem*, SIAM J. Matrix Anal. Appl., 26 (2005), pp. 640–659.
- [4] R. VAN BEEUMEN, *Rational Krylov Methods for Nonlinear Eigenvalue Problems*, PhD thesis, Department of Computer Science, KU Leuven, Belgium, 2015.
- [5] M. M. BETCKE AND H. VOSS, *Stationary Schrödinger equations governing electronic states of quantum dots in the presence of spin-orbit splitting*, Appl. Math., 52 (2007), pp. 267–284.
- [6] T. BETCKE, N. J. HIGHAM, V. MEHRMANN, C. SCHRÖDER, AND F. TISSEUR, *NLEVP: a collection of nonlinear eigenvalue problems*, ACM Trans. Math. Software, 39 (2013), pp. Art. 7, 28.
- [7] T. BETCKE AND H. VOSS, *A Jacobi-Davidson-type projection method for nonlinear eigenvalue problems*, Future Generation Comput. Syst., 20 (2004), pp. 363–372.
- [8] W. J. BEYN, *An integral method for solving nonlinear eigenvalue problems*, Linear Algebra Appl., 436 (2012), pp. 3839–3863.
- [9] D. M. DAY AND T. F. WALSH, *Quadratic Eigenvalue Problem*, Sandia Report SAND2007-2072, Sandia National Laboratories, Albuquerque, New Mexico 87185 and Livermore, California

94550, 2007.

[10] C. EFFENBERGER, *Robust successive computation of eigenpairs for nonlinear eigenvalue problems*, SIAM J. Matrix Anal. Appl., 34 (2013), pp. 1231–1256.

[11] C. EFFENBERGER AND D. KRESSNER, *Chebyshev interpolation for nonlinear eigenvalue problems*, BIT Numer. Math., 52 (2012), pp. 933–951.

[12] ———, *On the residual inverse iteration for nonlinear eigenvalue problems admitting a Rayleigh functional*, MATHICSE Technical Report Nr. 03.2014, EPFL - SB - MATHICSE, Station 8 - CH-1015 - Lausanne - Switzerland, Jan 2014.

[13] S. W. GAAF AND E. JARLEBRING, *The infinite bi-Lanczos method for nonlinear eigenvalue problems*, SIAM J. Sci. Comput., 39 (2016), pp. 898–919.

[14] B. GAVIN, A. MIEDLAR, AND E. POLIZZI, *FEAST eigensolver for nonlinear eigenvalue problems*, J. Comput. Sci., 27 (2018), pp. 107–117.

[15] S. GÜTTEL, R. VAN BEEUMEN, K. MEERBERGEN, AND W. MICHELS, *NLEIGS: a class of fully rational Krylov methods for nonlinear eigenvalue problems*, SIAM J. Sci. Comput., 36 (2014), pp. A2842–A2864.

[16] S. GÜTTEL AND F. TISSEUR, *The Nonlinear Eigenvalue Problem*, Acta Numer., 26 (2017), pp. 1–94.

[17] K. P. HADELER, *Mehrparametrische und nichtlineare Eigenwertaufgaben*, Arch. Ration. Mech. Anal., 27 (1967), pp. 306–328.

[18] E. JARLEBRING AND W. MICHELS, *Analyzing the convergence factor of residual inverse iteration*, BIT, 51 (2011), pp. 937–957.

[19] E. JARLEBRING, W. MICHELS, AND K. MEERBERGEN, *A linear eigenvalue algorithm for the nonlinear eigenvalue problem*, Numer. Math., 122 (2012), pp. 169–195.

[20] J. D. JOANNOPOULOS, S. D. JOHNSON, J. N. WINN, AND R. D. MEADE, *Photonic Crystals: Molding the Flow of Light*, second edition., Princeton University Press, 2008.

[21] D. KRESSNER, *A block Newton method for nonlinear eigenvalue problems*, Numer. Math., 114 (2009), pp. 355–372.

[22] V. N. KUBLANOVSKAYA, *On an approach to the solution of the generalized latent value problem for  $\lambda$ -matrices*, SIAM J. Numer. Anal., 7 (1970), pp. 532–537.

[23] P. LANCASTER, *A generalised Rayleigh quotient iteration for lambda-matrices*, Arch. Ration. Mech. Anal., 8 (1961), pp. 309–322.

[24] ———, *Lambda-matrices and vibrating systems*, Dover Publications, Inc., Mineola, NY, 2002. Reprint of the 1966 original [Pergamon Press, New York; MR0210345 (35 \#1238)].

[25] D. LU, Y. SU, AND Z. BAI, *Stability analysis of the two-level orthogonal Arnoldi procedure*, SIAM J. Matrix Anal. Appl., 37 (2016), pp. 195–214.

[26] D. S. MACKEY, N. MACKEY, AND F. TISSEUR, *Polynomial eigenvalue problems: theory, computation, and structure*, in Numerical algebra, matrix theory, differential-algebraic equations and control theory, Springer, Cham, 2015, pp. 319–348.

[27] V. MEHRMANN AND H. VOSS, *Nonlinear eigenvalue problems: a challenge for modern eigenvalue methods*, GAMM Mitt. Ges. Angew. Math. Mech., 27 (2004), pp. 121–152 (2005).

[28] V. MEHRMANN AND D. WATKINS, *Polynomial eigenvalue problems with hamiltonian structure*, Electron. Trans. Numer. Anal., 13 (2002), pp. 106–118.

[29] R. MENNICKEN AND M. MÖLLER, *Non-self-adjoint boundary eigenvalue problems*, vol. 192 of North-Holland Mathematics Studies, North-Holland Publishing Co., Amsterdam, 2003.

[30] W. MICHELS AND S.-I. NICULESCU, *Stability and stabilization of time-delay systems*, vol. 12 of Advances in Design and Control, Society for Industrial and Applied Mathematics (SIAM), Philadelphia, PA, 2007. An eigenvalue-based approach.

[31] A. NEUMAIER, *Residual inverse iteration for the nonlinear eigenvalue problem*, SIAM J. Numer. Anal., 22 (1985), pp. 914–923.

[32] K. MEERBERGEN R. VAN BEEUMEN AND W. MICHELS, *A rational Krylov method based on Hermite interpolation for nonlinear eigenvalue problems*, SIAM J. Sci. Comput., 35 (2013), pp. A327–A350.

[33] K. ROTHE, *Lösungverfahren für nichtlinearen Matrixeigenwertaufgaben mit Anwendungen auf die Ausgleichselementmethode*, PhD thesis, Universität Hamburg, Germany, 1989.

[34] A. RUHE, *Algorithms for the nonlinear eigenvalue problem*, SIAM J. Numer. Anal., 10 (1973), pp. 674–689.

[35] ———, *Algorithms for the nonlinear eigenvalue problem*, SIAM J. Numer. Anal., 10 (1973), pp. 674–689.

[36] ———, *Computing nonlinear eigenvalues with spectral transformation Arnoldi*, ZAMM, 76 (1996), pp. 17–20.

[37] ———, *A rational Krylov algorithm for nonlinear matrix eigenvalue problems*, Zap. Nauchn. Sem. S.-Peterburg. Otdel. Mat. Inst. Steklov. (POMI), 268 (2000), pp. 176–180, 245–246.

- [38] Y. SAAD, *Numerical Methods for Large Eigenvalue Problems-classics edition*, SIAM, Philadelphia, 2011.
- [39] T. SAKURAI AND H. SUGIURA, *A projection method for generalized eigenvalue problems using numerical integration*, in Proceedings of the 6th Japan-China Joint Seminar on Numerical Mathematics (Tsukuba, 2002), vol. 159, 2003, pp. 119–128.
- [40] K. SCHREIBER, *Nonlinear Eigenvalue Problems: Newton-type Methods and Nonlinear Rayleigh Functionals*, PhD thesis, Technische Universität Berlin, Germany, 2008.
- [41] H. SCHWETLICK AND K. SCHREIBER, *A primal-dual Jacobi-Davidson-like method for nonlinear eigenvalue problems*, TechRep ZIH-IR-0613, Technische Universität Dresden, Germany, 2006.
- [42] G. L. SLEIJPEN, A. G. L. BOOTEN, D. K. FOKKEMA, AND H. A. VAN DER VORST, *Jacobi-Davidson type methods for generalized eigenproblems and polynomial eigenproblems*, BIT, 36 (1996), pp. 595–633. International Linear Algebra Year (Toulouse, 1995).
- [43] S. I. SOLOV'EV, *Preconditioned iterative methods for a class of nonlinear eigenvalue problems*, Linear Algebra Appl., 415 (2006), pp. 210–229.
- [44] A. SPENCE AND C. POULTON, *Photonic band structure calculations using nonlinear eigenvalue techniques*, J. Comput. Phys., 204 (2005), pp. 65–81.
- [45] D. B. SZYLD AND F. XUE, *Efficient preconditioned inner solves for inexact Rayleigh quotient iteration and their connections to the single-vector Jacobi-Davidson method*, SIAM J. Matrix Anal. Appl., 32 (2011), pp. 993–1018.
- [46] ———, *Local convergence analysis of several inexact Newton-type algorithms for general nonlinear eigenvalue problems*, Numer. Math., 123 (2013), pp. 333–362.
- [47] ———, *Several properties of invariant pairs of nonlinear algebraic eigenvalue problems*, IMA J. Numer. Anal., 34 (2014), pp. 921–954.
- [48] F. TISSEUR AND K. MEERBERGEN, *The quadratic eigenvalue problem*, SIAM Rev., 43 (2001), pp. 235–286.
- [49] H. UNGER, *Nichtlineare Behandlung von Eigenwertaufgaben*, ZAMM Z. Angew. Math. Mech., 30 (1950), pp. 281–282.
- [50] R. VAN BEEUMEN, K. MEERBERGEN, AND W. MICHELIJS, *Compact rational Krylov methods for nonlinear eigenvalue problems*, SIAM J. Matrix Anal., 36 (2015), pp. 820–838.
- [51] H. VOSS, *A rational spectral problem in fluid-solid vibration*, Electron. Trans. Numer. Anal., 16 (2003), pp. 93–105 (electronic).
- [52] ———, *An Arnoldi method for nonlinear eigenvalue problems*, BIT, 44 (2004), pp. 387–401.
- [53] ———, *Numerical methods for sparse nonlinear eigenproblems*, in Proceedings of the XV-th Summer School on Software and Algorithms of Numerical Mathematics, Hejnice, 2003, I. Marek, ed., University of West Bohemia, Pilsen, Czech Republic, 2004, pp. 133–160.
- [54] ———, *Nonlinear Eigenvalue Problems - Chapter 60*, in Handbook of Linear Algebra, Second Edition, L. Hogben, ed., Discrete Mathematics and its Applications, Chapman & Hall/CRC, Boca Raton, FL, 2013, pp. 1063–1086.
- [55] B. WERNER, *Das Spektrum von Operatorscharen mit verallgemeinerten Rayleighquotienten*, Arch. Rational Mech. Anal., 42 (1971), pp. 223–238.
- [56] S. YOKOTA AND T. SAKURAI, *A projection method for nonlinear eigenvalue problems using contour integrals*, JSIAM Lett., 5 (2013), pp. 41–44.